

A Simplified Degradation Model for Nylon 6,6 Polymerization

D. D. STEPPAN,*¹ M. F. DOHERTY,² and M. F. MALONE²

¹Department of Polymer Science and Engineering, University of Massachusetts, Amherst, Massachusetts, 01003, and

²Department of Chemical Engineering, University of Massachusetts, Amherst, Massachusetts 01003

SYNOPSIS

A simplified reaction scheme for nylon 6,6 degradation that is consistent with all the published data is described. The degradation model has been incorporated into a flowing film polymerizer model with a distribution of residence times in order to predict molecular weight, amount of undegraded (amine and carboxyl) and degraded chain ends, and the extent of crosslinking. The outlet average molecular weight and water concentration come to steady state in about one mean residence time after a change in polymerizer operating conditions, whereas the degradation products continue to change slowly even after four residence times. Also, it is possible to choose the operating conditions of the polymerizer so the same molecular weight is produced at two different temperatures but with very different amounts of degradation products giving rise to products of significantly different quality.

INTRODUCTION

Thermal degradation can have a major impact on the quality of nylon 6,6 polymer. Small changes in the number of end groups (dye sites) can significantly change its dyability, whereas small amounts of crosslinking are very detrimental of fiber spinning. Therefore, the concentration of degraded ends in the typical industrial product must be very low and can only be measured accurately with very sensitive techniques. We have recently developed a comprehensive kinetic model for nylon 6,6 polymerization.¹ However, this kinetic model does not account for the side reactions that are significant at high temperatures and/or long residence times, which is a serious limitation. A reasonable degradation scheme along with accurate kinetic constants would add substantial realism to the model and significantly enhance its utility.

In this article, we seek to develop a degradation model that is both simple enough to be readily incorporated into our kinetic scheme and subsequently into a reactor model and that also accurately reflects

the effect of degradation on the nylon 6,6 product. It is not intended to reveal all degradation reactions that are occurring nor is it a detailed mechanistic study of their underlying chemistry. Our goal is to develop a simple, chemically reasonable degradation model that accurately describes the available degradation data in order to develop realistic process models for nylon 6,6.

It is well known that given sufficient time nylon 6,6 degrades and gels at high temperature even in the absence of oxygen. It is also well known that the degradation products include carbon dioxide, ammonia, and some cyclopentanone.² In this work we summarize a minimal set of reactions that can account for the formation of these products and for gelation. We have ignored degradation schemes that require oxygen so our task was considerably simplified.

This degradation description has been incorporated into a model for the dynamics of a flowing film polymerizer model.³ A velocity profile across the film gives rise to a distribution of residence times. Therefore, there is some material near the wall with residence times long enough to result in significant degradation at the high temperatures (250–290°C) typically encountered in the continuous production of nylon 6,6.⁴

* To whom correspondence should be addressed.

In this work we will evaluate extent of degradation for a range of operating conditions along with the relative time scales of the number average molecular weight to come to steady state as compared with that of the degradation products. This study provides a way to determine operating conditions that will minimize degradation.

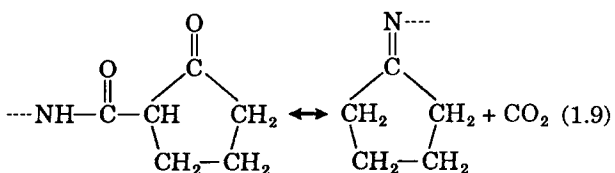
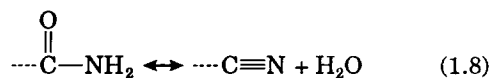
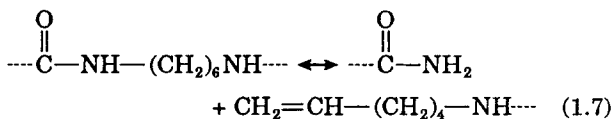
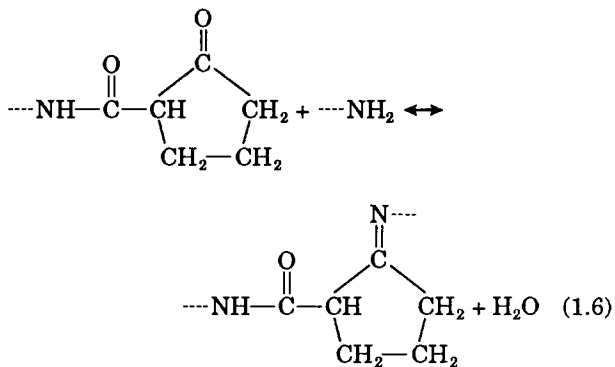
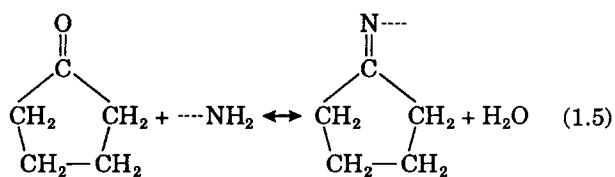
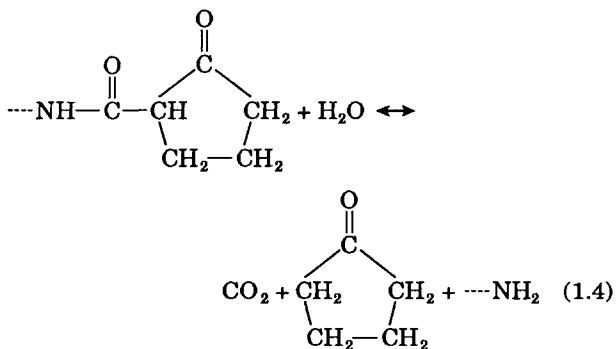
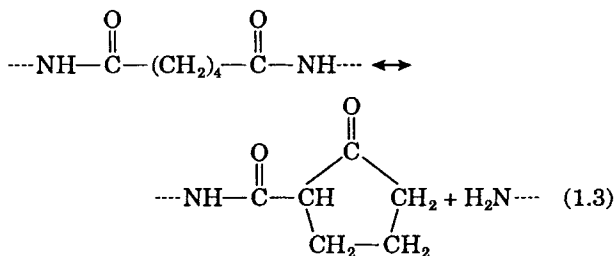
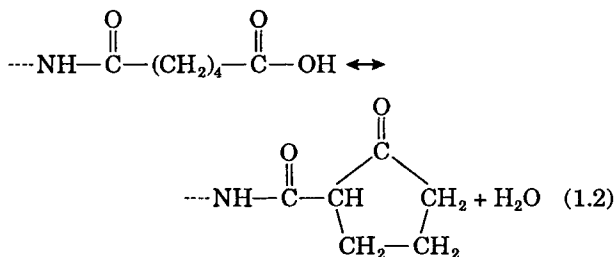
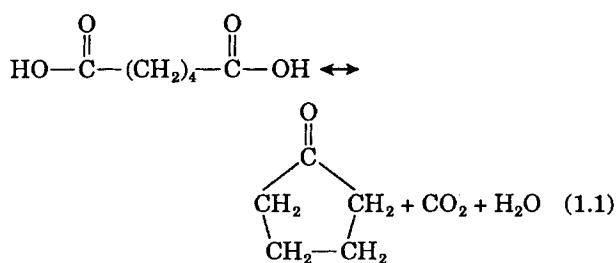
NYLON 6,6 DEGRADATION REACTIONS

Previous investigators have postulated a number of primary and secondary degradation reactions to ac-

count for the thermal instability of nylon 6,6. We summarize the more chemically feasible reactions in the following brief review of the literature.

At high temperature and under basic conditions, adipic acid is known to decompose into cyclopentanone, water, and carbon dioxide as shown by reaction (1.1) in Table I.⁵ Sweeney and Zimmerman² proposed an analog of reaction (1.1) that may take place both on the end of a nylon 6,6 chain and in the interior as shown in reactions (1.2) and (1.3). Achhammer, Reinhart and Kline⁶ have also suggested that the cyclopentyl chain end produced by reaction (1.3) may also continue to degrade as shown

Table I Nylon 6,6 Degradation Reactions



in reaction (1.4) to yield an amine end group, cyclopentanone and carbon dioxide. An amine end group can subsequently react with cyclopentanone to yield a Schiff base and water as shown in reaction (1.5).⁷ The cyclopentyl end group can also react with an amine end group to form a Schiff base and water as shown in reaction (1.6).⁸

Another possible degradation step is shown in reactions (1.7) and (1.8).^{2,9} In reaction (1.7), the weakest bond in the polyamide is broken at high temperature to form an olefinic end and a primary amide end. The latter is not stable and rapidly decomposes into a nitrile with the elimination of water by reaction (1.8). Wiloth and Schindler¹⁰ have shown that carbon dioxide and a Schiff base may be produced by a unimolecular mechanism shown in (1.9) from the cyclopentyl end group produced by reactions (1.2) and (1.3).

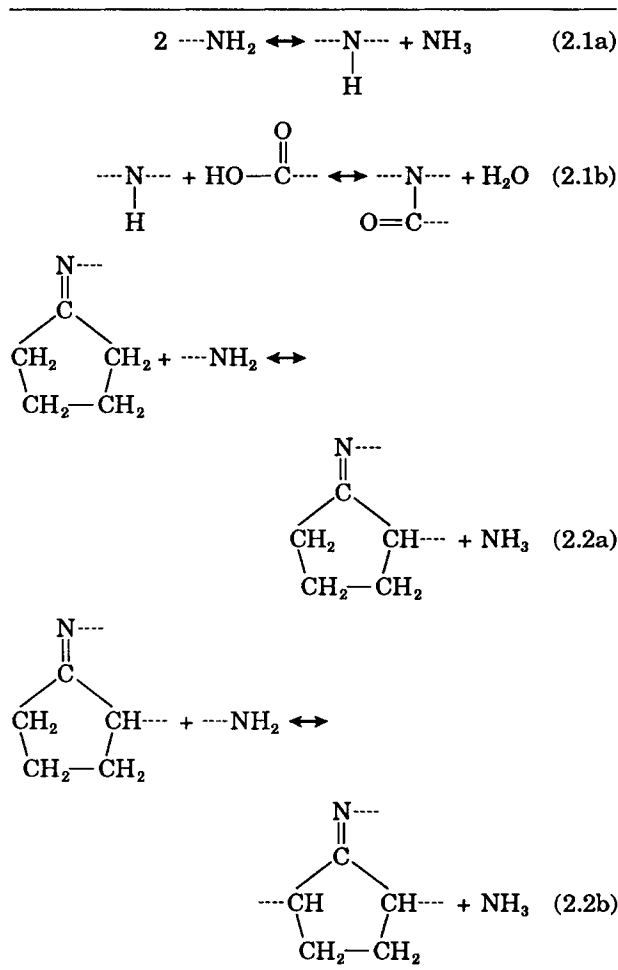
There is very little information on the origin of the crosslinks that are known to form in nylon 6,6 since there are so few and their chemical structure has not been unambiguously determined. In addition, it is very difficult to measure the number of crosslinks in any given sample because their relationship to measurable quantities is unknown (solution viscosity, titrable end groups). Nevertheless, two candidate crosslinking routes are shown in Table II. If a significant amount of water is present, there will be an appreciable amount of free amine and carboxyl groups from the reversible main amidation reaction. The amine end groups may combine and subsequently react with a carboxyl end group to form a crosslink as shown in reactions (2.1a and b) in Table II.¹¹ Wiloth¹² reports that the Schiff base formed via reactions (1.5) and (1.9) may subsequently react to form a variety of products including a crosslink as shown in (2.2a,b).

DEGRADATION STUDIES

Although there have been numerous studies on the degradation behavior of nylon 6,6 many do not contain enough quantitative data, about the time evolution of end groups and volatile gases, for the regression of kinetic constants necessary for the development of a degradation model. In the following section we summarize literature studies of nylon 6,6 degradation that have merit for the regression of kinetic constants in a degradation model.

Meacock¹³ studied how the number of amine and carboxyl end groups in nylon 6,6 changed with time at 293°C under 1 atm of steam; these data are shown in Figure 1. The number of amine end groups in-

Table II Nylon 6,6 Crosslinking Reactions



creases with time whereas the number of carboxyl end groups decreases.

Kamerbeek, Kroes, and Grolle⁹ also studied the thermal degradation of nylon 6,6 under nitrogen. Their data for the cumulative evolution of CO₂ and NH₃ from nylon 6,6 at 305°C are shown in Figure 2. We see that the polymer changes drastically over the course of the experiment since more than half of the nitrogen initially bound in amide linkages escapes as ammonia. Kamerbeek, Kroes, and Grolle⁹ emphasize the difficulty explaining the source of water required to drive reactions (1.4) and (2.1a) if these are the source of the carbon dioxide and ammonia. In addition, they found very little cyclopentanone and water in the evolving gases.

Edel and Etienne¹⁹ (1961) followed the amine end group, ammonia, and carbon dioxide evolution during the thermal degradation of nylon 6,6 under nitrogen. However, since they did not follow the carboxyl end-group evolution it is difficult to assess

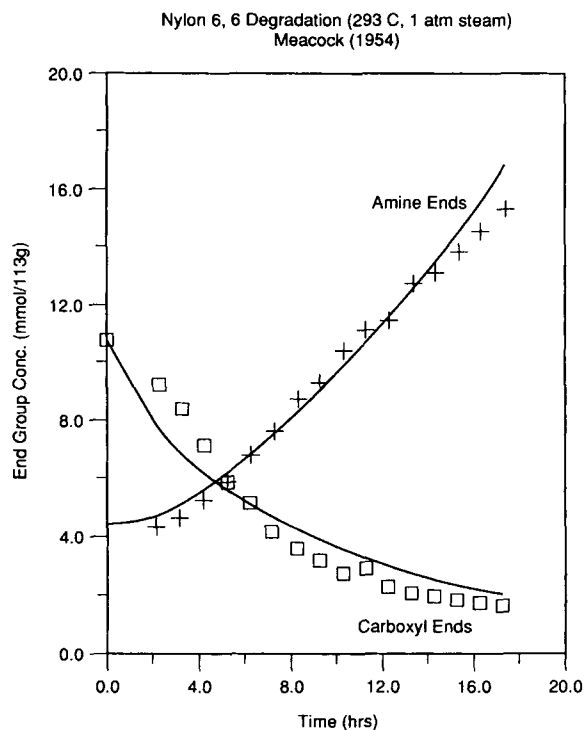


Figure 1 Nylon 6,6 degradation data (293°C and 1 atm steam) of Meacock¹³ and model fit.

what role the main amidation reaction played in the amine end-group evolution. This greatly reduces the utility of their data for our modeling purposes.

Peebles and Huffman¹⁴ found that the degradation behavior of nylon 6,6 was drastically altered if the degradation took place in a sealed reactor where the gaseous products were maintained over the melt compared with an open reactor (nitrogen gas maintained over the melt). In open reactors, the polyamide quickly discolored and subsequently crosslinked, becoming insoluble after 5–8 h at 282°C. However, in closed reactors the polymer remained white and crosslinked after about 50 h. The drastic difference between the two reactors was lessened when ammonia instead of nitrogen was passed through the reacting melt in the open reactor. The results of Peebles and Huffman¹⁴ suggest that the reaction that produces ammonia is reversible and/or that the ammonia reacts further when it remains in the melt.

In fact, Wiloth¹² suggests a mechanism where the ammonia reacts further in a closed reactor. He performed an extensive study on the thermal degradation in open and closed reactors. We will only analyze his data from open reactors (see Figs. 3 and 4) since our purpose is to describe commercial thin-film devices that correspond to this model of oper-

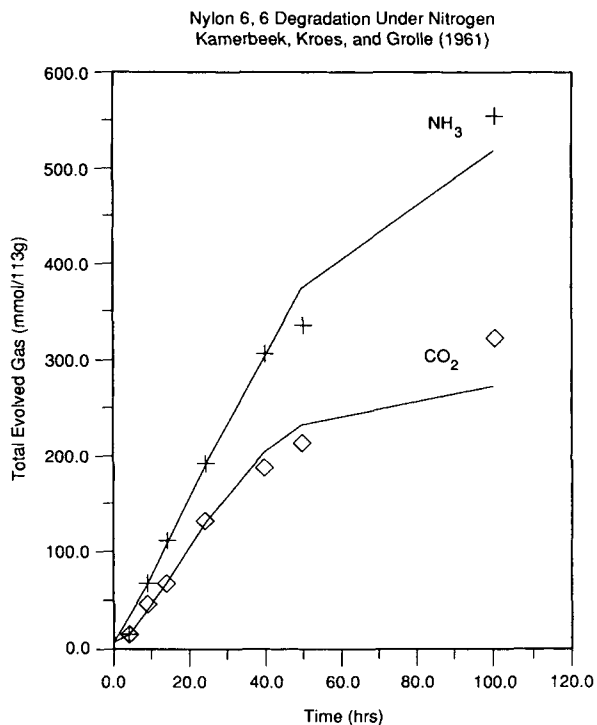


Figure 2 Nylon 6,6 degradation data (305°C under nitrogen) of Kamerbeek, Kroes, and Grolle⁹ and model fit.

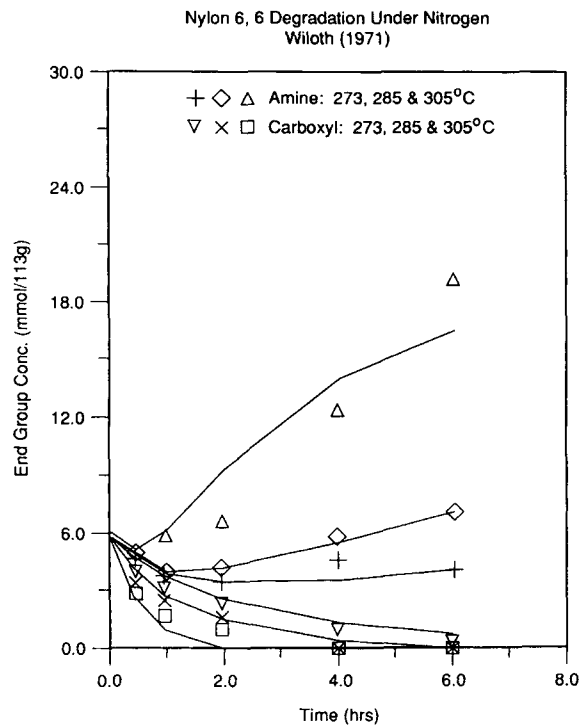


Figure 3 Nylon 6,6 end-group degradation data of Wiloth¹² and model fit.

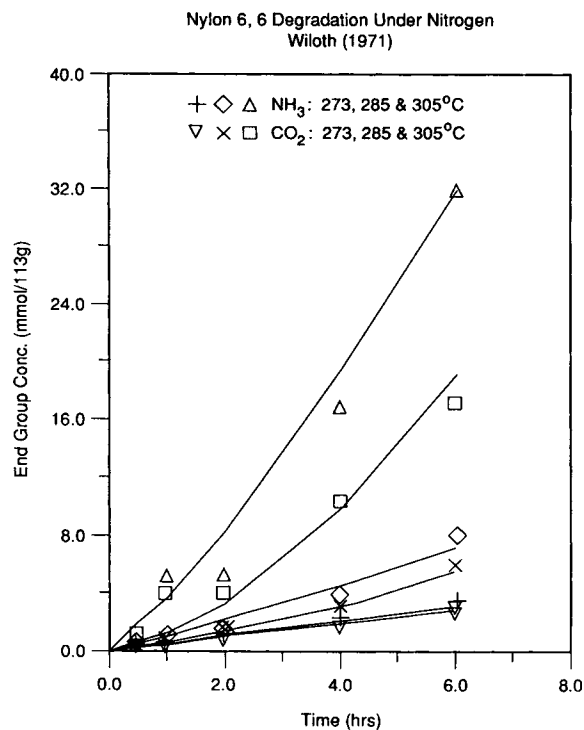


Figure 4 Nylon 6,6 volatile evolution data of Wiloth¹² and model fit.

ation. Furthermore, the potential problem with the reversibility of the reaction that produces ammonia is eliminated since the gaseous products (ammonia, carbon dioxide, and water) are rapidly removed from open reactors.

More recently, Ballistreri et al.⁷ studied the degradation of nylon 6,6 by direct pyrolysis into a mass spectrometer. By analyzing the degradation products, they concluded that the primary step in the thermal degradation was given by reaction (1.3) rather than (1.7). They found species with the cyclized end groups produced by (1.2) and (1.3), Schiff base species produced by (1.5) and (1.9), and the linkage produced by (2.2a).

DEGRADATION MODEL

We now describe a model that is consistent with the known reaction products and the minimum essential reactions from Tables I and II. From the data of Meacock¹³ and Wiloth¹² we know that reaction(s) that produce amine end groups and consume carboxyl end groups are necessary. Reactions (1.1), (1.2), and (2.1b) all consume carboxyl ends. However, reaction (1.1) is eliminated since the experiments all begin with high molecular weight starting

materials (high conversion > 98%), and the Flory distribution shows that negligible amounts of adipic acid are present. Reaction (1.2) is included in our model as the step that consumes carboxyl end groups. We have not included (2.1b) because, as discussed later, reaction (2.1a) is ruled out as a major step in the formation of ammonia.

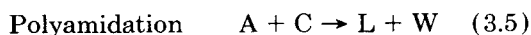
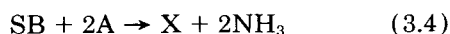
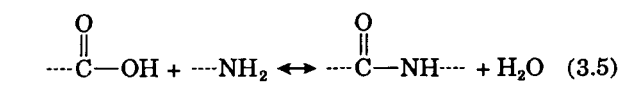
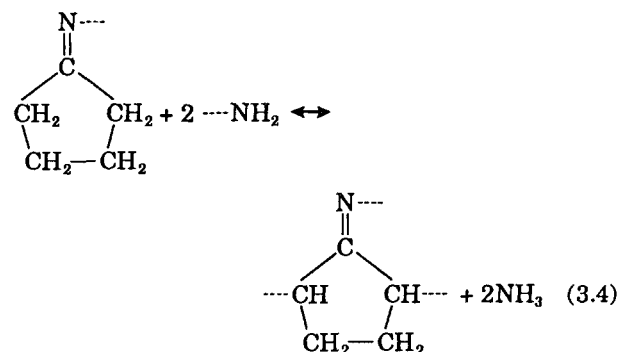
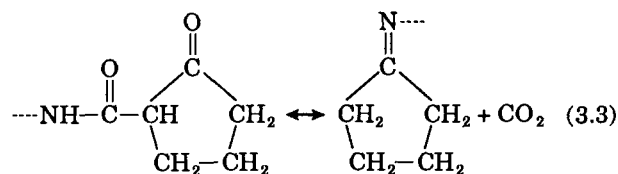
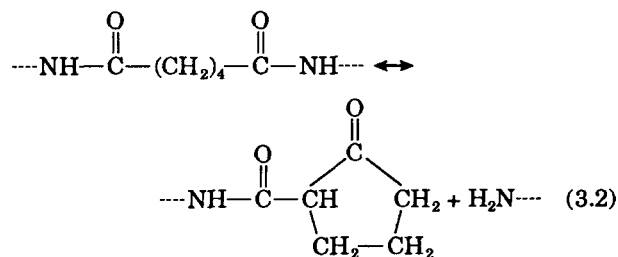
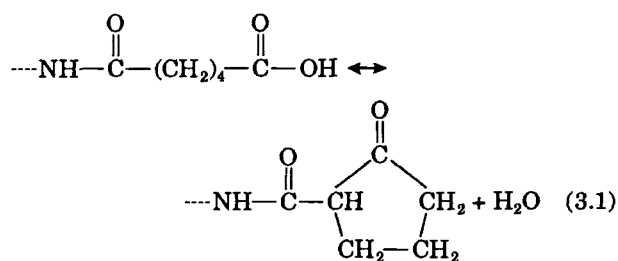
From the data of Kamerbeek, Kroes, and Grolle⁹ it is clear that not all of the CO₂ and NH₃ produced can be accounted for from reactions of the chain ends. For example, after 100 h, approximately 550 mmol/113 g of NH₃ and 330 mmol/113 g of CO₂ have been evolved, but at the start of the experiment only 10 mmol/113 g each of amine end groups and carboxyl end groups were present. Clearly, the amide linkage must be the source of much of the necessary oxygen and nitrogen. Reactions (1.1), (1.4), and (1.9) all produce CO₂. Reaction (1.1) is excluded for reasons mentioned previously. The reverse of the main amidation reaction produces a carboxyl end group, but we are realistically ignoring this reversibility for the analysis of the open reactor data where water is rapidly removed. Reaction (1.4) requires water whereas reaction (1.9) does not. Since we are assuming that the gaseous products are rapidly removed, reaction (1.9) will be used in the degradation model. Therefore, reaction (1.3) must be included as a source of stabilized end groups for consistency.

Ammonia is produced by reactions (2.1a) and (2.2a,b). Looking more closely at the data of Kamerbeek, Kroes, and Grolle,⁹ one sees that the final ammonia concentration of about 550 mmol/113 g cannot be generated solely by reaction (2.1a) since the initial concentration of amide linkages is 1000 mmol/113 g, which can produce at most 1000 amine end groups and subsequently 500 mmol/113 g of ammonia. Therefore, it is not sufficient to include only reaction (2.1a) in the model; however, it is sufficient to include only reaction (2.2), which we have done in keeping with our goal of developing the simplest realistic scheme. In addition, these reactions give rise to the crosslink that is consistent with the data of both Kamerbeek, Kroes, and Grolle⁹ and Wiloth¹².

The degradation model is summarized in Table III along with the main amidation reaction. They are abbreviated as



Table III Nylon 6,6 Degradation Model



where C refers to a carboxylic acid end group, SE to a stabilized (or cyclized) end group, W to a water molecule, L to an amide linkage, A to an amine end group, CO₂ refers to carbon dioxide, SB to a Schiff base and X to a crosslink.

The rates of the reaction steps (3.1–3.5) are assumed to be given by

$$R_1 = C_T k_1 X_C \quad (1)$$

$$R_2 = C_T X_L (k_2 + k_{2C} X_A) \quad (2)$$

$$R_3 = C_T k_3 X_A X_{SE}^a \quad (3)$$

$$R_4 = C_T k_4 X_{SB}^b X_A \quad (4)$$

$$R_5 = C_T k_{app} \left(X_A X_C - \frac{X_L X_W}{K_{app}} \right) \quad (5)$$

where ($C_T = C_A + C_C + C_L + C_W + C_{SE} + C_{SB} + C_X$), $X_A = C_A/C_T$, etc., and reaction (3.2) has been treated as an end-group catalyzed reaction as recommended by Twilley.⁸ We have also assumed that reaction (2.2b) is very rapid compared to (2.2a). Therefore, the rate-limiting step for reaction (3.4) is given by reactions (2.2a). The rate of (2.2a) is given by $C_T k_{2.2a} X_{SB}^b X_A$ is eq. (4). The rate and equilibrium constants for the amidation reaction are known functions of temperature and composition.¹

The mass balances for the various species are given by

$$\frac{dC_A}{dt} = R_2 - 2R_4 - R_5 \quad (6)$$

$$\frac{dC_C}{dt} = -R_1 - R_5 \quad (7)$$

$$\frac{dC_L}{dt} = -R_2 + R_5 \quad (8)$$

$$\frac{dC_W}{dt} = R_1 + R_5 \quad (9)$$

$$\frac{dC_{SE}}{dt} = R_1 + R_2 - R_3 \quad (10)$$

$$\frac{dC_{NH_3}}{dt} = 2R_4 \quad (11)$$

$$\frac{dC_{CO_2}}{dt} = R_3 \quad (12)$$

$$\frac{dC_{SB}}{dt} = R_3 - R_4 \quad (13)$$

$$\frac{dC_X}{dt} = R_4 \quad (14)$$

Since we have assumed that the rate of removal of the volatile components in the reacting mixture is very rapid, eqs. (9), (11), and (12) really reflect the rate at which these products are evolved as gas per unit volume of the reacting mixture. The concentration of water, carbon dioxide, and ammonia is assumed to be negligible in the analysis of the data in Figures 1–4. The sole exception to this is for the

closed reactor data of Meacock where we estimate the water concentration as a constant from the correlation of Ogata¹⁵ for the equilibrium mole fraction of water in the polymer as a function of the partial pressure of water in the gas phase.

The temperature dependence of the rate constants was fit with the usual Arrhenius form by optimizing an integral analysis.

$$k = k_0 \exp \left[\frac{-E_{\text{app}}}{R} \left(\frac{1}{T} - \frac{1}{T_0} \right) \right] \quad (15)$$

The resulting set of kinetic parameters is shown in Table IV.

The predicted end-group concentrations are compared to the data of Wiloth in Figure 3. The fit is reasonably good at all temperatures for the amine end groups. However, the carboxyl end-group predictions are slightly high, especially for the highest temperature data. This is because the assumption of a zero water concentration is not exactly correct, and the carboxyl end groups are consumed by the main amidation reaction rather than degradation reaction (3.1) in this simulation. Consequently, it is difficult to estimate the reaction rate of reaction (3.1) from the open reactor experiments because it is masked by the main amidation reaction. Therefore, we have estimated it from the closed reactor data of Meacock, which is under a constant finite water concentration so that the amidation reaction is near equilibrium throughout the experiment. The parameters obtained from open reactor data can accurately describe the amine end-group evolution in open reactors but cannot do the same for closed reactors. In order to properly account for the effect of the reversible main amidation reaction on the concentration of carboxyl end groups in addition to reaction (3.1), we have fit the amine end-group evolution in the closed reactor with an empirical function of the amide linkage concentration and the amine end-group concentration. The results are

Table IV Kinetic Parameters for Nylon 6,6 Degradation

Model Reaction	k_0 (liter/h)	E_{app} (cal/mol)	T_0 (°C)	
1	0.06	30,000	293	
2	0.005	30,000	305	
2 (catalyzed)	0.32	30,000	305	
3	0.35	10,000	305	$a = 0.1$
4	10.0	50,000	305	$b = 0.3$

shown in Figure 1 (in Figs. 1–4 the points represent the data and the lines the model fit). We are unable to estimate an activation energy for reaction (3.1) since Meacock presents data only at a single temperature. However, since (3.1) is so similar to (3.2) we have set the two activation energies equal.

The data of Wiloth on the evolution of NH_3 and CO_2 are shown in Figure 4 along with the model predictions, which seem to be as accurate as justified by the data at the three temperatures investigated. The fit of the long time data of Kamerbeek, Kroes, and Grolle⁹ for NH_3 and CO_2 evolution is shown in Figure 2. Again, the model provides an accurate quantitative estimate for the amount of each of the components except, perhaps, at very long times.

INCORPORATION OF THE DEGRADATION SCHEME INTO THE FLOWING FILM MODEL

We have incorporated this degradation model into our flowing film polymerizer model.³ The flowing film geometry is shown in Figure 5. In this model, which is typically operated at higher water concentrations and lower temperatures, water is no longer assumed to be instantly removed but instead is allowed to diffuse out of the film. The evolution equations for the nonvolatile components and water, in dimensionless form, are

$$\frac{\partial C_A}{\partial t} = \phi^2 (r_2 - 2r_4 - r_5) - \left(\frac{\phi^2}{\text{Da}} \right) v_y \frac{\partial C_A}{\partial Y} \quad (16)$$

$$\frac{\partial C_C}{\partial t} = \phi^2 (-r_1 - r_5) - \left(\frac{\phi^2}{\text{Da}} \right) v_y \frac{\partial C_C}{\partial Y} \quad (17)$$

$$\frac{\partial C_L}{\partial t} = \phi^2 (-r_2 + r_5) - \left(\frac{\phi^2}{\text{Da}} \right) v_y \frac{\partial C_L}{\partial Y} \quad (18)$$

$$\begin{aligned} \frac{\partial C_W}{\partial t} = \phi^2 (r_1 + r_5) - \left(\frac{\phi^2}{\text{Da}} \right) v_y \frac{\partial C_W}{\partial Y} \\ + \frac{\partial}{\partial Z} \left(\frac{\hat{C}}{1-x} \frac{\partial x}{\partial Z} \right) \end{aligned} \quad (19)$$

$$\frac{\partial C_{\text{SE}}}{\partial t} = \phi^2 (r_1 + r_2 - r_3) - \left(\frac{\phi^2}{\text{Da}} \right) v_y \frac{\partial C_{\text{SE}}}{\partial Y} \quad (20)$$

$$\frac{\partial C_{\text{SB}}}{\partial t} = \phi^2 (r_3 - r_4) - \left(\frac{\phi^2}{\text{Da}} \right) v_y \frac{\partial C_{\text{SB}}}{\partial Y} \quad (21)$$

$$\frac{\partial C_X}{\partial t} = \phi^2 r_4 - \left(\frac{\phi^2}{\text{Da}} \right) v_y \frac{\partial C_X}{\partial Y} \quad (22)$$

where the concentrations and reaction rates are now dimensionless, $x = C_W/\hat{C}$ is the mole fraction of wa-

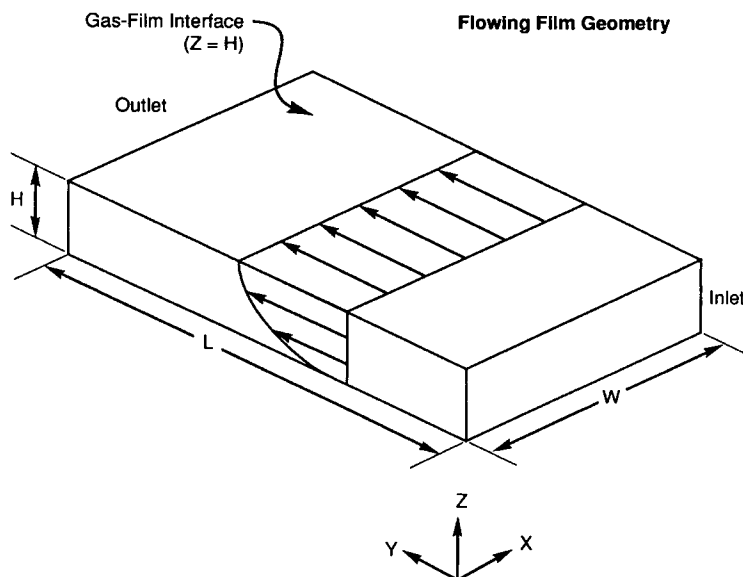


Figure 5 Flowing film geometry.

ter, $\hat{C} = C_A + C_C + C_L + C_W + C_{SB} + C_{SE} + C_X$ is the dimensionless total molar concentration, and v_y is the dimensionless fluid velocity in the flow direction. Only the water balance contains a diffusion term since it is the only species we allow to diffuse out of the film. All the other species are part of the large polymer molecules that we have assumed do not diffuse. The boundary condition for the water balance are that the concentration of water is constant at the gas–film interface and the flux of water is zero ($\partial x/\partial z = 0$) at the solid wall–film interface.

The variables in the model have been scaled with respect to a characteristic time, length, concentration, reaction rate constant, and velocity. We have chosen the characteristic time as the ratio of the square of the film thickness to the diffusivity (H^2/D), where the diffusivity is taken at the temperature of the system. The characteristic length is taken to be the film height (H) and the characteristic concentration is the initial value for water (C_W^0). For the characteristic reaction rate constant we use the value of main amidation reaction rate constant at 200°C as both the water and carboxyl end-group mole fractions approach zero ($k_{app}^0 = 2.926/h$). The characteristic velocity is the film average velocity $\langle v_y \rangle$. In deriving eqs. (4) and (5), we have assumed that the reacting mixture can be treated as a binary solution to describe the diffusion, that the mutual diffusivity depends on temperature but not on composition, that the polymer does not diffuse, that water diffuses in the Z direction, and that diffusion is negligible compared to convection in the Y direction.

The Damkohler number (Da) is defined¹⁷ as

$$Da = \frac{L/\langle v_y \rangle}{1/k_{app}^0} = \frac{t_{residence}}{t_{reaction}} \quad (23)$$

where $\langle v_y \rangle$ and L are the average velocity and the axial length of the film, k_{app}^0 is the reference apparent reaction rate constant for nylon 6,6 polyamidation. The Thiele modulus (ϕ^2) is¹⁸

$$\phi^2 = \frac{H^2/D}{1/k_{app}^0} = \frac{t_{diffusion}}{t_{reaction}} \quad (24)$$

where H is the film height and D the mutual diffusivity of the water–polymer mixture.

We have estimated the total concentration of polymer molecules (C_p) by

$$C_p = \frac{C_A + C_C + C_{SE} + C_{SB} - C_X}{2} \quad (25)$$

in these modeling studies. This expression is approximate, although it becomes exact if there is at most one crosslink in any polymer molecule. Therefore, it is valid for small amounts of crosslinking. The balance equations have been integrated by the method of lines.¹⁸

RESULTS

We have evaluated extent of degradation for some typical operating conditions in order to estimate the amount of degraded material in the industrial prod-

uct. In addition, we have determined the relative time scales of the number averaged molecular weight to come to steady state as compared with that of the degradation products for a reasonable change in reactor throughput to demonstrate why certain product properties may continue to change even after the number averaged molecular weight has reached steady state. The complex interplay of the effects of reaction temperature and residence time on the amount of degradation are also studied in order to determine operating conditions that will minimize degradation.

We have previously shown³ that typical values of the Thiele modulus range from 0.1 to 10.0 corresponding to film thickness of 0.2 to 1.7 cm. Typical values of the Damkohler number range from 0.05 to 5 corresponding to residence times from 1 to 100 min. We have evaluated the effect of changing the Damkohler number from 2.5 to 3.0 at a constant Thiele modulus of 1.0 (film thickness of 0.5 cm) and reactor temperature of 270°C. This corresponds to increasing the mean residence time in the reactor from 50 to 60 min, an increase of 20%. The evolution of the cup-mixed average of different species as a function of intervals of the mean residence time is shown in Figure 6. Figure 6(a) shows that the cup-mixed number average molecular weight of the effluent increases from 10,800 to 11,440 g/mol, the concentration of amine ends decreases from 9.7 to 9.1 mmol/113 g, and the concentration of carboxylic acid ends decreases from 9.3 to 8.7 mmol/113 g. In Figure 6(b) we can see that water concentration decreases from 25.1 to 24.3 mmol/113 g, the stabilized end concentration increases from 0.53 to 0.64 mmol/113 g, the crosslink concentration increases from 0.6 to 0.7 mmol/113 g, and the Schiff base end concentration (which has been multiplied by 1.5 for visibility in the figure) increases from 0.4 to 0.48 mmol/113 g.

In Figure 7 we show the effect of increasing the reactor temperature to 280°C for the same case as in Figure 6. Figure 7(a) shows that the cup-mixed number average molecular weight of the effluent increases from 11,300 to 11,900 g/mol, the concentration of amine ends decreases from 9.2 to 8.7 mmol/113 g, and the concentration of carboxylic acid ends decreases from 8.9 to 8.3 mmol/113 g. In Figure 7(b) we can see that water concentration decreases from 25.9 to 24.8 mmol/113 g, the stabilized end concentration increases from 1.25 to 1.5 mmol/113 g, the crosslink concentration increases from 1.15 to 1.3 mmol/113 g, and the Schiff base end concentration (which has been multiplied by 5 in the figure) increases from 0.19 to 0.21 mmol/113 g.

Comparing Figure 6 and 7 reveals that the steady-

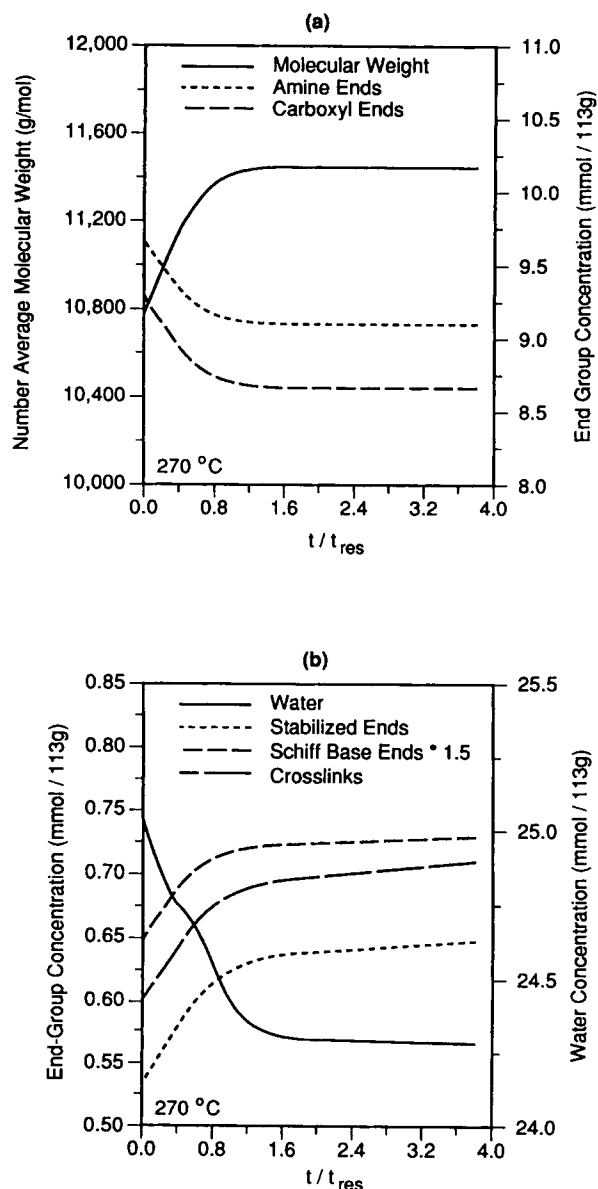


Figure 6(a) The time evolution of the effluent average number average molecular weight, amine, and carboxyl end-group concentrations for the flowing film model as the Damkohler number is changed from 2.5 to 3.0 at a Thiele modulus of 1.0 and 270°C.

Figure 6(b) The time evolution of the effluent average water, stabilized end-group, Schiff base end-group and crosslink concentrations for the flowing film model as the Damkohler number is changed from 2.5 to 3.0 at a Thiele modulus of 1.0 and 270°C.

state concentration of stabilized ends and crosslinks approximately doubles with the increase in temperature while the concentration of Schiff base ends decreases by a factor of 2. In addition, the molecular weight, amine end, carboxyl end, and water concentration come to steady state in about 1.2 residence

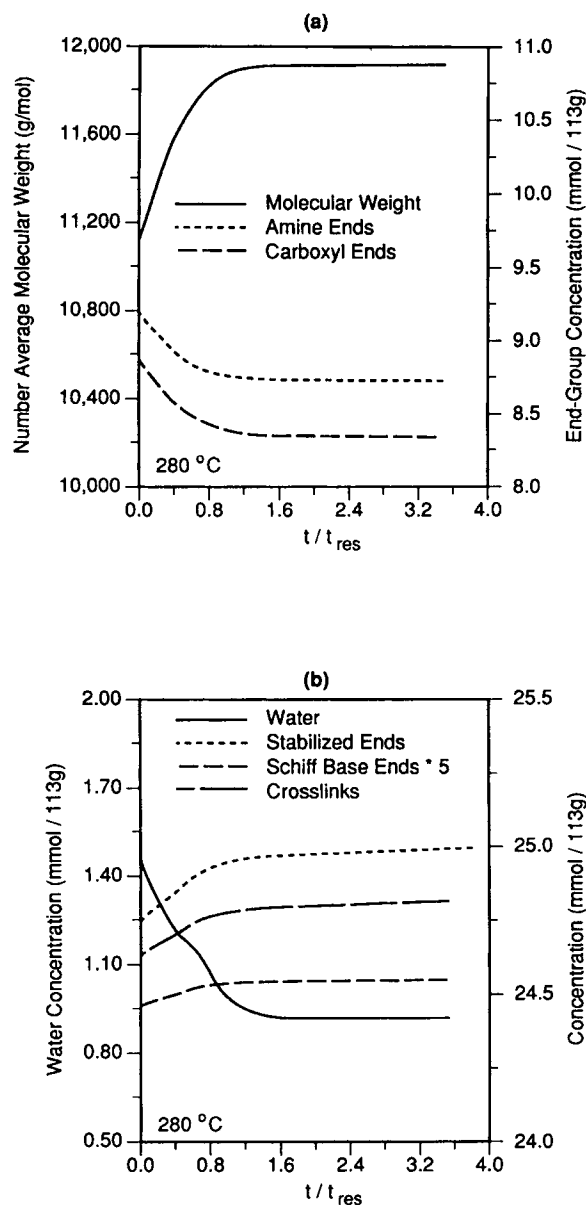


Figure 7(a) The time evolution of the effluent average number average molecular weight, amine, and carboxyl end-group concentrations for the flowing film model as the Damkohler number is changed from 2.5 to 3.0 at a Thiele modulus of 1.0 and 280°C.

Figure 7(b) The time evolution of the effluent average water, stabilized end-group, Schiff base end-group, and crosslink concentrations for the flowing film model as the Damkohler number is changed from 2.5 to 3.0 at a Thiele modulus of 1.0 and 280°C.

times (1.2 h) at both temperatures. However, the system is not a steady state. The stabilized end, Schiff base end, and crosslink concentrations continue to increase slowly, for much longer times. Therefore, the molecular weight and water concen-

tration may appear to be at steady state, the (small) concentration of degraded products changes over much longer time scales. This is because the slow moving material with longer residence times near the stationary reactor wall has not reached steady state and contributes to changing the small amounts of degraded product but does not affect the molecular weight.

It is useful to try to counterbalance the increase of molecular weight resulting from the increased mean residence time by decreasing the reaction temperature. Figure 8(a) shows the effect of decreasing the reaction temperature from 270 to 262°C for the same increase in residence time as in Figure 6(a). The molecular weight goes through a minimum after about one-half a residence time and then regains its initial value. This minimum occurs because the material in the reactor undergoes an instantaneous decrease in temperature and concomitant instantaneous decrease in amidation rate whereas the increase in the mean residence time is not instantly realized by any of the material already in the reactor at the time the average velocity (mean residence time) is reduced since it has already traversed part of the reactor at a faster velocity (shorter residence time). Therefore, the material in the reactor when the operating conditions are changed has a different thermal/residence time history than the material before or after. After slightly more than one residence time this effect has disappeared, and the molecular weight regains its initial value. Similar behavior is displayed by the amine ends. The carboxyl ends decrease somewhat due to the longer residence time and the relatively low activation energy of reaction (3.1).

The evolution of water and degradation products for the same simultaneous increase in residence time and decrease in operating temperature are shown in Figure 8(b), which should be compared with the isothermal case in Figure 6(b). The outlet water concentration shows similar overall behavior, decreasing in both cases. However, the higher operating temperature yields a slightly higher outlet water concentration because water is a product of both the main amidation (3.5) and stabilized end-group formation (3.1) reactions, which are accelerated as the temperature is increased. The concentration of Schiff based end groups also shows similar behavior, increasing in both cases. However, the Schiff base concentration is higher (about 20%) at the lower temperature. In addition, the concentration of stabilized end groups and crosslinks show very different behavior under the two operating conditions. In the isothermal case [Fig. 6(b)] they both increase significantly (by about 15%) whereas they both de-

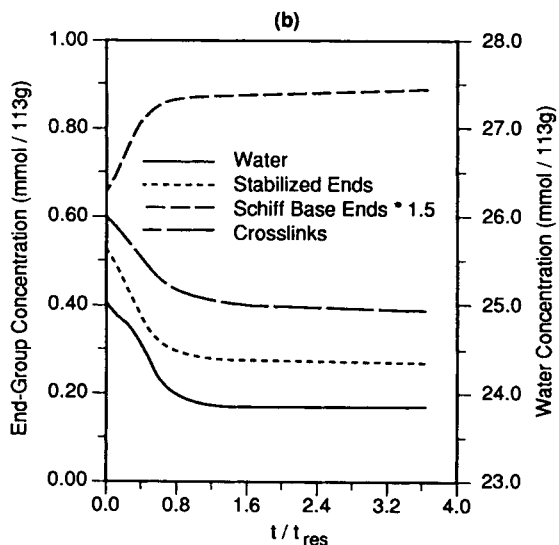
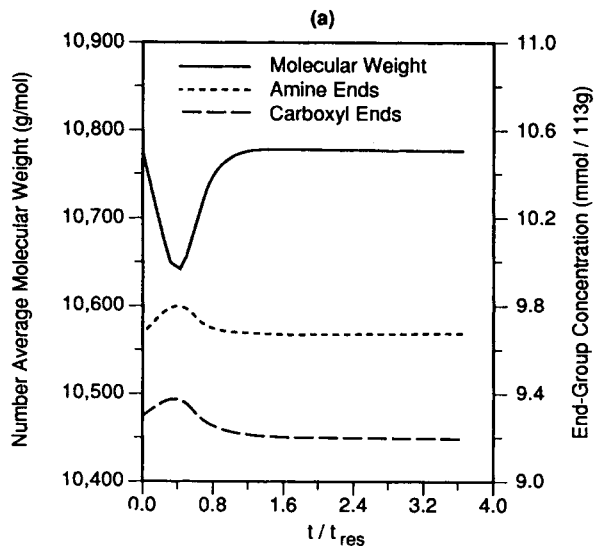


Figure 8(a) The time evolution of the effluent average number average molecular weight, amine, and carboxyl end-group concentrations for the flowing film model as the Damkohler number is changed from 2.5 to 3.0 and the temperature reduced from 270 to 262°C at a Thiele modulus of 1.0.

Figure 8(b) The time evolution of the effluent average water, stabilized end-group, Schiff base end-group, and crosslink concentrations for the flowing film model as the Damkohler number is changed from 2.5 to 3.0 and the temperature reduced from 270 to 262°C at a Thiele modulus of 1.0.

crease (by about 35%) at the lower temperature [Fig. 8(b)]. Therefore, it is important to decide which is the most important for maintaining the desired product properties.

The effect of decreasing the reactor temperature from 280 to 268°C as the mean residence time is increased is shown in Figure 9, which should be compared to the isothermal case in Figure 7. Very similar conclusions may be drawn by comparing

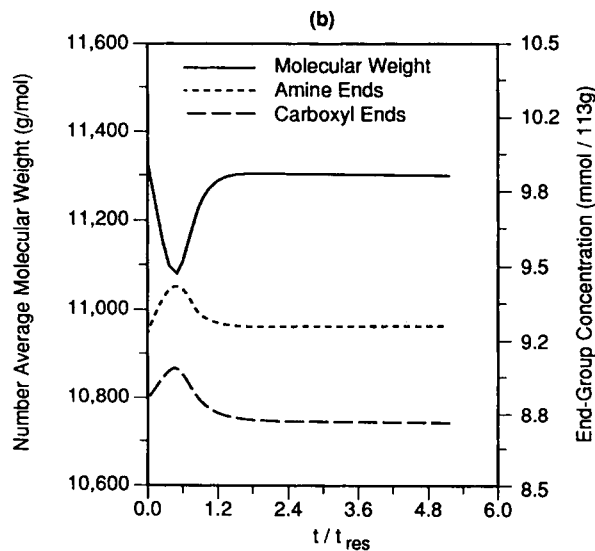
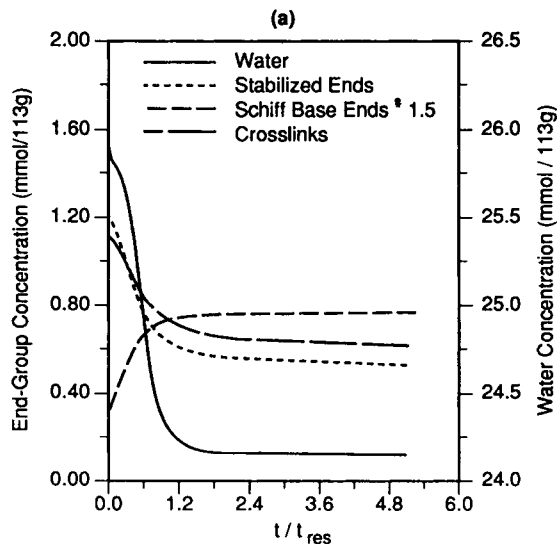


Figure 9(a) The time evolution of the effluent average number average molecular weight, amine, and carboxyl end-group concentrations for the flowing film model as the Damkohler number is changed from 2.5 to 3.0 and the temperature reduced from 280 to 268°C at a Thiele modulus of 1.0.

Figure 9(b) The time evolution of the effluent average water, stabilized end-group, Schiff base end-group, and crosslink concentrations for the flowing film model as the Damkohler number is changed from 2.5 to 3.0 and the temperature reduced from 280 to 268°C at a Thiele modulus of 1.0.

Figures 9 and 7. The molecular weight and amine end concentration regain their initial values after one residence time, and the carboxyl end concentration decreases to a slightly lower value. The water and degradation products all change significantly from their initial values with the water and Schiff base end groups showing qualitatively similar behavior under the two operating conditions. The stabilized end group and crosslink concentrations show qualitatively different evolution, decreasing at the lower operating temperature and increasing in the isothermal case.

CONCLUSIONS

Figures 6–9 illustrate two important points. Even though the flowing film reactor may be operated under two different operating conditions to produce a product with essentially identical molecular weights, the final products can contain very different amounts of degraded products and may therefore display significantly different end-use properties in some applications. Therefore, the optimal operating policy will depend on the desired final product characteristics (molecular weight, end-group balance, etc.). Second, this model is suitable for dynamic control studies. For example, it might be used to investigate how the operating temperature and pressure (the pressure in the gas phase affects the water concentration at the gas–film interface) can be manipulated to counterbalance throughput changes.

Many possible degradation mechanisms are postulated in the literature for nylon 6,6. It is not feasible or necessary to include all the side reactions and/or to measure their kinetic constants in order to describe the performance of typical industrial reactors. We have hypothesized a minimal subset of reactions that can be used to estimate the degradation, and we have regressed kinetic constants for them. We expect that this is a representative degradation mechanism that would be sufficient for estimating the low levels of byproducts that can be permitted in the typical industrial product.

We have shown that the flowing film model predicts that the outlet average molecular weight and water concentration come to steady state in about one mean residence time after a change in polymerizer operating conditions whereas the degradation products continue to change slowly even after four residence times. In addition, we have shown that it is possible to choose the operating conditions of the polymerizer so the same molecular weight is

produced at two different temperatures but with very different amounts of degradation products giving rise to two products of significantly different quality.

We are grateful for financial and technical support from E. I. Du Pont de Nemours and Co.

Notation

A	Amine end group
C	Carboxyl end group
\hat{C}	Molar density ($C_W + C_P$), dimensionless
C_i	Concentration of component i , dimensionless [before Eq. (17) mol/L]
C_T	Total molar density for nylon 6,6 amidation ($C_T = C_A + C_C + C_L + C_W + C_{SE} + C_{SB} + C_X$), dimensionless [before Eq. (17) mol/L]
D	Diffusivity, cm^2/s
Da	Damkohler number ($k_{\text{app}}^0 L / \langle v_y \rangle$), dimensionless
E_{app}	Apparent activation energy, cal/mol
H	Film height, cm
k_i	Forward reaction rate constant for reaction i , h^{-1}
k_{app}^0	Reference apparent forward reaction rate constant, 2.926 h^{-1}
K_{app}	Apparent equilibrium constant ($X_L X_W / X_A X_C$), dimensionless
L	Amide linkage or reactor length, m
M_n	Number average molecular weight, g/mol
r_i	Reaction rate, dimensionless
R_i	Reaction rate of component i , mol/l h
SB	Schiff base end group
SE	Stabilized or cyclized end group
t	Time, dimensionless
v_y	Velocity, dimensionless
$\langle v_y \rangle$	Average velocity, m/h
W	Water molecular, Eq. (1)
x	Binary mole fraction of water (C_i / \hat{C}), dimensionless
X_i	Mole fraction of component i for nylon 6,6 amidation (C_i / C_T), dimensionless
X	Crosslink
ϕ^2	Thiele modulus ($H^2 k_{\text{app}}^0 / D$), dimensionless

REFERENCES

1. D. D. Steppan, M. F. Doherty, and M. F. Malone, *J. Appl. Polym. Sci.*, **33**, 2333 (1987).
2. W. Sweeney and J. Zimmerman, "Polyamides," *The*

- Encyclopedia of Polymer Science and Technology*, H. F. Mark, N. G. Gaylord, and N. M. Bikales, (Eds.), Wiley-Interscience, New York, 1964, Vol. 10, pp. 483-597.
3. D. D. Steppan, M. F. Doherty, and M. F. Malone *Ind. Eng. Chem. Res.*, **28**, 1324 (1989).
 4. U.S. Pat., 3,900,450 (1975) (to Dupont),
 5. R. T. Morrison and R. N. Boyd, *Organic Chemistry*, 3rd ed., Allyn and Bacon, Boston, 1973, Chapter 20, p. 667.
 6. B. G. Achhammer, F. W. Reinhart, and G. M. Kline, *J. Appl. Chem.*, **1**, (1951) 301.
 7. Ballistreri, D. Garozzo, M. Giuffrida, and G. Montaudo, *Macromolecules*, **20**, (1987) 2991.
 8. I. C. Twilley, in discussion of *Thermal Degradation of Some Polyamides*, in Soc. Chem. Ind. Monograph 13, 1961, p. 388.
 9. B. Kamerbeek, G. H. Kroes, and W. Grolle, *Thermal Degradation of Some Polyamides*, in Soc. Chem. Ind. Monograph 13, 1961, p. 357.
 10. F. Wiloth and E. Schindler, *Chem. Ber.*, **100**, (1967) 2373.
 11. D. A. S. Ravens and J. E. Sisley, "Cleavage Reactions," in *Chemical Reactions of Polymers*, E. M. Fetters, (Ed.) Wiley-Interscience, New York, 1964, p. 610.
 12. F. Wiloth, *Makromol. Chem.*, **144**, (1971) 283.
 13. G. Meacock, *J. Appl. Chem.*, **4**, (1954) 172.
 14. L. H. Peebles and M. W. Huffman, *J. Polym. Sci.*, **9**, (1971) 1807.
 15. N. Ogata, *Makromol. Chem.*, **42**, 52 (1960).
 16. K-H. Lin and H. C. Van Ness, in *Chemical Engineers' Handbook* R. H. Perry and C. H. Chilton (Eds.), McGraw-Hill, New York (1973), Chapter 4.
 17. J. M. Smith, *Chemical Engineering Kinetics*, 2nd ed., McGraw-Hill, New York, 1970, Chapter 11, pp. 430-432.
 18. W. H. Press, B. P. Flannery, S. A. Teukosky, and W. T. Vetterling *Numerical Recipes: The Art of Scientific Computing*, Cambridge University Press, New York, 1986, esp. Chapter 17.
 19. G. Edel and H. Ettiene, *Bull. Inst. Text. Fr.*, **23**(142), 343 (1969).

Received September 1988

Accepted March 8, 1990